Journal of Computational Neuroscience 18, 131–149, 2005

Velocity-Based Planning of Rapid Elbow Movements Expands the Control Scheme of the Equilibrium Point Hypothesis

MASATAKA SUZUKI*
Department of Psychology, Kinjo Gakuin University, Nagoya 463-8521, Japan
msuzuki@kinjo-u.ac.jp

YOSHIHIKO YAMAZAKI
Department of Computer Science and Engineering, Graduate School of Engineering, Nagoya Institute of Technology, Nagoya 466-8555, Japan

Received May 17, 2004; Revised September 21, 2004; Accepted September 24, 2004

Action Editor: Alessandro Treves

Abstract. According to the equilibrium point hypothesis of voluntary motor control, control action of muscles is not explicitly computed, but rather arises as a consequence of interaction between moving equilibrium position, current kinematics and stiffness of the joint. This approach is attractive as it obviates the need to explicitly specify the forces controlling limb movements. However, many debatable aspects of this hypothesis remain in the manner of specification of the equilibrium point trajectory and muscle activation (or its stiffness), which elicits a restoring force toward the planned equilibrium trajectory. In this study, we expanded the framework of this hypothesis by assuming that the control system uses the velocity measure as the origin of subordinate variables scaling descending commands. The velocity command is translated into muscle control inputs by second order pattern generators, which yield reciprocal command and coactivation commands, and create alternating activation of the antagonistic muscles during movement and coactivation in the post-movement phase, respectively. The velocity command is also integrated to give a position command specifying a moving equilibrium point. This model is purely kinematics-dependent, since the descending commands needed to modulate the visco-elasticity of muscles are implicitly given by simple parametric specifications of the velocity command alone. The simulated movements of fast elbow single-joint movements corresponded well with measured data performed over a wide range of movement distances, in terms of both muscle excitations and kinematics. Our proposal on a synthesis for the equilibrium point approach and velocity command, may offer some insights into the control scheme of the single-joint arm movements.

Keywords: equilibrium point hypothesis, velocity command, stiffness, visco-elasticity

1. Introduction

Much of the appeal of the equilibrium point hypothesis of voluntary motor control is its potential to be an alternative to carrying out the complex computations of inverse dynamics for deriving control actions (Bizzi et al., 1992; Feldman et al., 1990). Despite the many variations in the equilibrium point model, a common postulate is that a higher motor center generates descending commands encoding a temporal sequence of signals that specifies the equilibrium position and stiffness of the limb. The stiffness transforms a displacement from the equilibrium position into an elastic restoring force. In theory, therefore, when the

*To whom all correspondence should be addressed.

equilibrium point shifts, the limb is at all times attracted by the elastic restoring force toward the instantaneous equilibrium point.

The inherent elastic properties of active muscles have provided the neurophysiological basis for the equilibrium point hypothesis (Bizzi et al., 1984; Hogan, 1985; Rack and Westbury, 1969), yet there is still a distance from this hypothesis to the large volume of experimental data. During arm movements, for example, the motor command modulates the muscle activation in a systematic manner, depending on the changes of movement parameters such as moving different distances at different speeds (Hoffman and Strick, 1990, 1993; Gottlieb, 1996; Pfann et al., 1998). However, the manner in which the commands for muscles are scaled to generate the class of movement speeds or distances has not been taken into account in the previous models. Also, muscle activation as an implicit determinant of stiffness in this hypothesis is not constant, but varied in time even in a single stroke of movement (Gomi and Kawato, 1997; Osu et al., 2001; Osu and Gomi, 1990). An adjustment of appropriate muscle activation (or stiffness) to realize the planned trajectory over the movement could be a complex task for the control system, similar to that expected in solving inverse dynamics problems (Gomi and Kawato, 1997). Therefore, a simple but flexible framework in specifying both the muscle excitation (or stiffness) and equilibrium point shift would be needed in this theory.

The purpose of the present paper was to extend the framework of this hypothesis by assuming that the control signals in the higher motor center are programmed in a velocity-dependent manner. This assumption is based on empirical findings about the oculomotor system, which has a program to compute and combine velocity and position commands (Robinson, 1989). Similar to the oculomotor system, the planned velocity command in the model constitutes muscle control inputs, and its time-integral specifies the equilibrium position of the limb. The system dynamics depend on the parametric specifications of the velocity command, without need for explicit computations of muscle control actions. This means that elastic and damping forces are both provided as an implicit interaction among the moving equilibrium point, mechanical properties of active muscles and kinematics. The model predictions were examined through comparisons to experimental data. A human elbow single-joint acting upon a pair of antagonistic muscle groups was used in the simulations and experiments.

2. Experiments

2.1. Apparatus and Procedures

Four subjects with unknown history of neurological disorders gave informed consent to participate in the experiments. Each subject was seated in a straight-back chair, and the right arm was placed on a single-joint manipulandum located in the horizontal plane at the shoulder joint level. The forearm was pronated at 90° with all digits and the thumb naturally palmar-abducted. The elbow joint center was positioned exactly above the vertical axis of rotation of the manipulandum. Then three portions of the forearm and hand (i.e., the wrist, the midpoint of the forearm segment and the lateral sides of the palm) were clamped between pairs of vertical mechanical stops, and fixed to the manipulandum by bracing to prevent independent movement between the segments and manipulandum. Elbow angles were defined relative to the upper arm. The angle was 0° with the arm fully extended and increased with elbow flexion.

The subject faced a cathode ray oscilloscope, 1m away, which displayed the elbow angle as a movable line, and initial and target angles as two horizontal lines. The subject had to adjust the elbow angle to the initial position of 70°. After relaxing the entire arm, the subject made an elbow flexion movement to one of three target angles set at 17° (small; *S*), 34° (medium; *M*) and 50° (Large; *L*) from the initial position. The subject was instructed to flex the elbow as fast and accurately as possible. The subject was told to perform the movement in a single stroke and not to attempt to correct the movement once initiated. The subject was given a 10-min practicing period before the data collection to become acclimated to the manipulandum and the general task requirements. A block of each target distance consisted of 5 trials, and 15 trials (three blocks) were collected in total. The order of blocks for each movement distance was randomized between subjects. Before each new block, the subjects practiced 5 trials to become familiar with each movement distance. However, once the test trial began, the next 5 recording trials (one block) were performed consecutively with an inter-trial rest of 10 sec. A few minutes of rest were allowed between blocks.

For three subjects the same *L* movements were performed with an additional inertial load of 0.0513 kgm^2 created by a weight fixed to the distal end of the manipulandum ('load condition'). In addition, for one subject

L movements were performed with an additional instruction to decrease the magnitude of the coactivation, that is, 'relax immediately after the start of movement' ('relaxed condition') (Yamazaki et al., 1994). When following this instruction, the subject did not have to fix his arm at the terminal phase of movement, allowing the arm to deviate from the target position with time.

Electromyographic (EMG) signals were recorded from two single- and double-joint elbow muscles. The single-joint elbow muscles were the biceps long head (BL) and triceps lateral head (TLa), and the double-joint elbow muscles were the biceps short head (BS) and triceps long head (TLo). A series of test maneuvers involving free movements and isometric force adjustments were carried out to verify the electrode placement on the muscle belly (Gribble and Ostry, 1998). After amplification with a band-pass of 20–1000 Hz, EMG signals were sampled at 1 kHz and stored along with joint displacement data, which was measured from a potentiometer (EP45, Japan Servo Co., Ltd.), connected to the lower end of the axis of rotation of the manipulundam. The LabVIEW Development System (National Instru. Co.) was used for data collection.

2.2. *Data Analyses and Simulations*

In each trial, the onset of EMG from either of the agonist muscles was compared from the first clear separation from baseline, and the earlier one was specified with a resolution of 1msec. These onsets were written to the file header and served to align the data for EMGs and kinematics. Joint velocity and acceleration were computed by numerically differentiating the position signals.

The measured displacement data averaged over 15 trials was used to determine the best-fit model in the simulations. The model includes a single rectangular velocity (V) command specifying the average velocity of the desired movement. The second order differential of the V command and its integral define the equilibrium point shift and muscle control inputs (i.e., EMGs), respectively (see Model section). For each movement condition, two parameters (t_2 and a) of the V command were varied inversely to preserve the same initial and final positions of the simulated displacement curve as those of the measured curve. The period of this adjustment of the simulated curves was from the start of the first agonist EMG to the end of the terminal oscillation of the measured curve. The least square error method was used in selecting the best combination of a and t_2 values, and a correlation coefficient for this best-fit model was calculated ($p < 0.001$). Under the best-fit parameters for each movement condition, correlation between the measured and simulated curves for velocity was calculated.

The scaling constants of the measured EMGs were determined from averaged data of the L movements in the normal condition. After the best combination of a and t_2 values in the V command were given, the averaged EMGs recorded from four muscles were scaled individually to the simulated EMG data using the least square error method. This was done for the relationship between a modeled flexor EMG and measured EMG from each of two flexor muscles (BS and BL), and between a modeled extensor EMG and measured EMG from each of two extensor muscles (TLo and TLa). The time window of this adjustment was the same as that used in the simulation of a corresponding displacement curve. It should be noted that the scaling constant of individual muscles in the L movements was fixed to simulate measured EMGs in smaller movement, load and relaxation conditions of the same subject. A correlation analysis was also carried out to evaluate the model prediction of EMGs. These off-line analyses and simulations were carried out using a computerized routine coded in Matlab (MathWorks, Inc.).

3. The Model

3.1. *Planned Variables*

The trajectory determination task is both space- and time-dependent. Therefore, the position (P) and velocity (V) measures at the stage of planning must not be mutually exclusive, such that

$$P = P_0 + Vt$$
$$\text{where} \quad V(t) = \begin{cases} 0 & t < t_0 \\ \pm a & t_0 \le t \le t_2 \\ 0 & t > t_2 \end{cases} \tag{1}$$

P_0 is the initial joint position. t_2 is the movement time and movement starts at $t = t_0$. V is the average velocity of movement, such that V and P are rectangular and ramp shaped, respectively (Fig. 1A and B, respectively). The V signal is specified by a set of three parameters: direction ($\pm$), height (a) and width (t_2) (Fig. 1A). Positive and negative signs for a represent elbow flexion and extension, respectively. As follows, the V signal elicits a first strong EMG volley in the

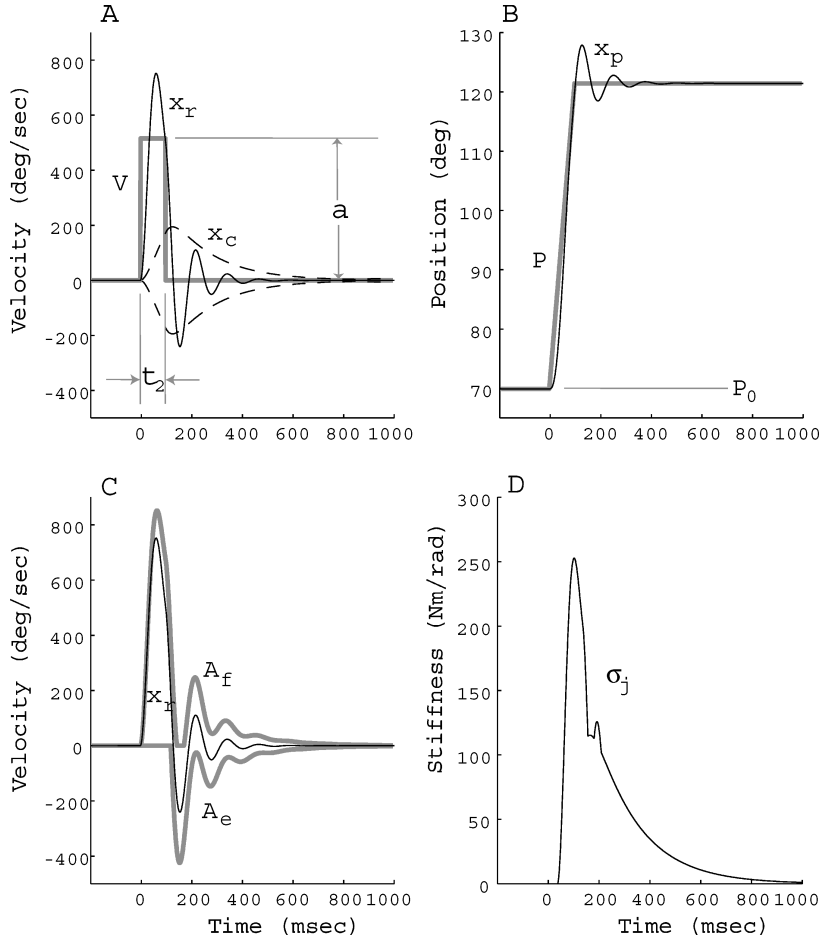

Figure 1. Relationships among planned command V, descending commands (x_r, x_c and x_p), EMGs (A_f and A_e) and joint stiffness (σ_j). A: V command (half-tone line) and its transformation into two muscle control inputs, reciprocal command x_r (solid line) and coactivation command x_c (broken lines). Note that x_r is asymmetric, while x_c is symmetric and bi-directional. B: P (half-tone line) is the time integral of the V command in A. x_p (solid line) denotes the descending command specifying the joint equilibrium position. C: Relationship between x_r and EMGs. A_f and A_e are flexor and extensor EMGs, respectively. D: joint stiffness (σ_j) represented by the sum of muscle stiffness in (6).

agonist muscles (Freund and Büdingen, 1978; Ghez, 1979; Hoffman and Strick, 1990, 1993), analogous to that called a 'pulse' known in the oculo-motoneuron (MN) discharges (e.g., Robinson, 1970, 1989).

3.2. Descending Commands

We hypothesized that at the output stage of motor commands, the planned V signal is used to scale muscle control inputs and joint equilibrium position. As for the former, two pattern generators are assumed to transform the V command into two descending commands, the reciprocal command (x_r) and the coactivation command (x_c), which are characterized by underdamped and overdamped actions, respectively (Fig. 1A)(for details, see below)

$$V \rightarrow \begin{cases} \begin{pmatrix} x_r \\ x_c \end{pmatrix} \\ x_p \left(= \int x_r dt + P_0 \right) \end{cases} \tag{2}$$

where the command x_r is integrated to provide the joint equilibrium position command x_p, which is regarded as the underdamped response of the P (Fig. 1B). Although the relationship between the commands x_r and x_p is rewritten as a set of differential equations, we choose the integral form for reasons of biological realism in the oculomotor system (Robinson, 1989).

The assumption of separate command generators for x_r and x_c in (2) is based on behavioral evidence that human subjects have the ability to independently vary the magnitude of reciprocal activation and coactivation (Yamazaki et al., 1994). The presence of motor units that display 'common drive' to the antagonistic muscles is consistent with the idea of centrally specified coactivation of antagonistic muscles (DeLuca and Mambrito, 1987). Supporting evidence from electrophysiological studies suggests that the command oriented cell assemblies (i.e., reciprocal activation and coactivation) could be formed elsewhere in the cerebellar circuit involving the precentral cortex (Humphry and Reed, 1981) and cerebellum (Frysinger et al., 1984).

During fast single-joint movements, the EMG patterns of the antagonistic muscles consist of a series of three or more partially overlapped alternating bursts of activity, followed by a prolonged much lower coactivation lasting after the movement end (e.g., Gribble and Ostry, 1998; Milner 2002; Suzuki et al., 2001; Yamazaki et al., 1994) (for our results, see Figs. 3 and 4). Among these, the following (3) assumes that the command x_r constitutes the rhythm and amplitude of alternating bursts of the antagonistic muscles, while x_c elevates and overlaps these alternating bursts during movement and leads to post-movement coactivation (Fig. 1C) (for details, see the next section)

$$m_i\ddot{x}_i + c_i\dot{x}_i + k_i x_i = V \quad \text{for } i = r, c \tag{3}$$

where m_i, c_i and k_i are constants. Subscripts r and c denote reciprocal and coactivation commands, respectively. By choosing appropriate values of m_i, c_i and k_i, this system creates command x_r or x_c in response to a common rectangular pulse command V as follows.

In reproducing command x_r, the m_r, c_r and k_r values in (3) are set at 1, 25 and 2700, respectively, and are fixed across the subjects. These parameters yield the underdamped sinusoidal response of command x_r with a natural frequency of 8.02 Hz and a damping ratio of 0.24 (Fig. 1A). In flexion movement shown in Fig. 1A, for example, x_r consists of an initial strong positive half-cycle and a subsequent much weaker negative half-cycle, followed by the gradual decay of sinusoidal oscillation at a relatively constant rate (Wadman et al., 1979). The autonomous rhythmicity of the command x_r may not be attributable to a particular neural substrate(s), e.g., a central pattern generator in the lower motor center (Grillner, 1981). Rather it may be ascribed to intrinsic properties of the higher motor circuits, which provide a predictive reciprocal activation pattern for the agonist and antagonist muscles with minor contribution of reflexes (Braitenberg et al., 1997; Brooks and Thach, 1981).[1]

The command x_c is characterized as overdamped decay (i.e., the response is purely exponential) that is bi-directional (Fig. 1A). Since EMG coactivation appears to be blended with the reciprocal activation during movement, it is difficult to specify the time-varying pattern of the coactivation command from EMG signals. Milner (2002) has shown that during slower wrist single-joint movements, coactivation as a gradually decreasing tonic activation level of the antagonistic muscles is manifested behind the small reciprocal bursts. Indirect evidence may be obtained from joint stiffness profiles during limb movements, showing that phasic components are superimposed on a gradually decreasing component toward the movement end (Gomi and Kawato, 1997; Latash and Gottlieb, 1991; Osu et al., 2001) (for our model, see Fig. 1D). This offset elevation of joint stiffness may be due to the underlying coactivation, which increases once and then decays gradually toward the complete relaxation of antagonistic muscles after the movement end. To satisfy this hypothetical wave property, the m_c, c_c and k_c values in (3) were set at 1, 40 and 200, respectively, and were fixed across the subjects.

The relationship between commands x_r and x_c is linear, such that their response amplitudes are scaled by a common scaling factor a, the amplitude of the V command in (1). This implies a speed-related linkage between command x_r and x_c as has been postulated in empirical and simulation studies. In a perturbation study, Bennet (1993) showed that in elbow single-joint movements an increase in joint stiffness is accompanied by an increase in joint velocity. Similarly, in modeling studies, the coactivation command during movements must increase monotonically as a function of movement velocity in order to increase joint speed and joint stiffness in parallel (Gribble et al., 1998; Lan and Crago, 1994). Suzuki et al. (2001) have shown that muscle coactivation following movement end increases with joint velocity as well as the phasic initial agonist EMG burst at the instant of movement.

3.3. Muscle Activations

The commands x_r and x_c create activation for a pair of antagonistic muscles. The command x_c increases the simultaneous excitation of antagonistic muscles in

opposite directions, while command x_r interacts with x_c by its facilitatory and inhibitory drives (Fig. 1A and 1C) (see below)

$$A_f = [x_r + x_c]^+; \quad A_e = [x_c - x_r]^+ \tag{4}$$

where A is the muscle excitation (i.e., EMG) and subscripts f and e denote flexor and extensor, respectively. Square brackets $[\ ]^+$ imply that both A_f and A_e must be positive or zero. This means that at the limiting time when the absolute value of x_r for antagonist muscles is equal to or exceeds the level of x_c, the activity of the opposing muscle is zero (non-negative). In order to relate the temporal relationship between reciprocal command x_r and the alternating behavior of the mutual antagonistic muscles, the A_e burst is inverted hereafter.

As shown in Fig. 1A, the first half-cycle of x_r sums up x_c in the agonist (flexor) side [left form in (4)] while reducing x_c of the antagonist (extensor) side [right form in (4)]. Thus x_c elevates the agonist (A_f) burst more than in cases where the same x_r is exerted without x_c (Fig. 1C). In this phase, x_r is strong enough to completely suppress the opposing muscle (A_e) and elicits a single agonist activation (A_f). After a peak of the first half-cycle of x_r, depression of the antagonist muscle becomes incomplete (Fig. 1A), leading to an earlier initiation of the first A_e burst, which overlaps with the end of the first A_f burst (Fig. 1C). After the second half-cycle of x_r, overlap or coactivation of the antagonistic muscles becomes manifest as the oscillatory amplitude of x_r decays with time (Fig. 1C). The background neuronal mechanism of this reciprocal interaction is that command x_r for the agonist motoneurons (MNs) interacts with the antagonist muscle by inhibiting its MNs by way of spinal interneurons. This scheme can be expected from parallel (or collateral) descending command pathways, which simultaneously excite and inhibit the agonist and antagonist MNs, respectively (Jankowska et al., 1976; Rothwell et al., 1984).

3.4. *Transformation into Torque*

With reference to the previous equilibrium point models (e.g., Lan and Crago, 1994), joint torque is defined as

$$\tau = \sigma_j(x_p - x - \delta\dot{x}^{\phi}) \quad \text{if } \dot{x} \le 0, \quad \dot{x}^{\phi} = -|\dot{x}|^{\phi} \tag{5}$$

where τ is net joint torque; command x_p specifies the equilibrium position, and x is the current joint position. σ_j is joint stiffness defined as the sum of flexor muscle stiffness σ_f and extensor muscle stiffness σ_e (see below). The last term $\sigma_j\delta\dot{x}^{\phi}$ is damping torque, where δ is the scaling constant for the damping coefficient ($\sigma_j\delta$), and $\dot{x}$ is the current joint velocity. Subscript ϕ less than 1.0 denotes that damping torque is the fractional power function of joint velocity (see below). Positive and negative signs for τ represent flexor and extensor torque, respectively. In the absence of a damping term, joint torque is represented by the spring-like behaviors tuned by neuromuscular activity (Hogan, 1985), which is supported by empirical observations (Bizzi et al., 1984; Rack and Westbury, 1969). Since these experiments involved completely deafferented muscles, this spring-like behavior is not contingent upon the presence of sensory feedback information.

3.5. *Stiffness*

Muscle stiffness is assumed to be proportional to the level of muscle activation

$$\sigma_f(t) = \kappa A_f(t - d); \quad \sigma_e(t) = \kappa A_e(t - d) \tag{6}$$

where κ is the constant coefficient transforming muscle excitation into muscle stiffness and represents a magnitude parameter related to the torque generating capability for a set of antagonistic muscles; d is electromechanical delay assumed to be constant at 40 msec (Latash and Goodman, 1994). Since muscle activation in (4) is a velocity measure, κ has the unit of Nm·s/rad^2. An implicit assumption for κ is that the biomechanical parameters (e.g., averaged moment arm and physiological cross sectional area of synergist muscles) of the opposing muscles are constant and symmetric.

The derivation of κ was based on the recent studies of EMG-based estimation of joint stiffness (Osu et al., 2001; Osu and Gomi, 1999). Osu et al. (2001) have shown that in both postures and reaching movements of the upper limb, joint stiffness computed from the linear relationship between surface EMG and joint torque correlated well with joint stiffness measured directly by applying mechanical perturbation. In our model, a scaling constant of 6.27 Nm/rad (i.e., stiffness per unit torque: SPUT) developed in Osu et al. (2001) for predicting joint stiffness from torque measure, was first applied to the measured torque data averaged for 15 trials of largest (50°) movements.[2] In order to reproduce this stiffness measure, κ was set around 17.0, and varied among subjects (Table 1). As shown in Fig. 1,

Table 1. Correlation coefficients of the best-fit simulations of four subjects.

		Subject			
		1	2	3	4
I		0.121	0.115	0.129	0.135
κ		17.0	16.8	15.5	18.0
			x		
	L	0.999	0.999	0.998	0.998
		0.998		0.992	0.998
	M	0.999	0.997	0.990	0.993
	S	0.999	0.997	0.984	0.993
			$\dot{x}$		
	L	0.996	0.995	0.966	0.985
		0.985		0.955	0.980
	M	0.981	0.956	0.945	0.953
	S	0.994	0.985	0.940	0.971
			BS		
	L	0.967	0.905	0.964	0.441
		0.957		0.978	0.315
	M	0.980	0.959	0.848	0.505
	S	0.954	0.827	0.848	0.921
			BL		
	L	0.939	0.330	0.937	0.549
		0.951		0.948	0.462
	M	0.952	0.369	0.937	0.792
	S	0.969	0.792	0.863	0.875
			TLo		
	L	0.602	0.423	0.705	0.634
		0.609		0.805	0.279
	M	0.609	0.555	0.883	0.533
	S	0.884	0.935	0.879	0.500
			TLa		
	L	0.869	0.621	0.642	0.297
		0.698		0.579	0.114
	M	0.667	0.476	0.803	0.570
	S	0.936	0.813	0.826	0.895

Underlined values are for the loaded condition.

for example, the simulated EMGs in 1C multiplied by a κ value of 17.0 generate a joint stiffness curve in 1D which peaks once at 251.0Nm/rad [= 17 Nm·s/rad^2 × 14.78 rad/s (= 847 deg/s)], followed by a gradual decrease toward complete relaxation of the muscles. This peak corresponded to that of the reference stiffness, for which the measured torque peak was 40 Nm [i.e., 251.0 Nm/rad =6.27 × 40 Nm].

3.6. Damping

In the definition of the damping term in (5), the dependence of the damping coefficient on the muscle stiffness (or muscle activation) is first defined as $\sigma_j\delta$, since the damping coefficient increases with muscle stiffness (Cannon and Zahalak, 1982; Kearnery and Hunter, 1990). By choosing an appropriate δ value, $\sigma_j\delta$ yields movements with good agreement to experimentally observed trajectories at slow and moderate speeds of movement (Flash, 1987). Flash (1987) chose δ values in the range of 0.05 to 0.125 s in the simulation of multi-joint arm reaching movements performed over a workspace. However, the effectiveness of a constant δ value is questionable at faster movements, since speed-related attenuation of the damping torque is assumed from the combined effects of muscle contractile properties and reflex (Gielen and Houk, 1984; Milner and Cloutier, 1998). Therefore, as a second option, we define the damping torque as consisting of a linear element $\sigma_j\delta$ and a nonlinear element ϕ. We set δ and ϕ values at 0.125 s and 0.63, respectively. The δ value of 0.125 s is the upper most used by Flash (1987), but in (5) the fractional power ϕ attenuates the speed-related elevation of the damping torque in the higher velocity range. When velocity is 10 rad/s, for example, the damping torque derived from Flash's linear model is 1.25 σ_j, while that in our model is 0.553 σ_j. The latter value is compatible to the damping torque when the lowest value of δ (0.05 s) in Flash (1987) was used. The value of ϕ is slightly elevated compared to that used in previous modeling studies (Barto et al., 1999; Wu et al., 1990) because a low fractional power (0.3–0.5) may be largely ascribed to the velocity reflex (Gielen and Houk, 1984), which is not taken into account in the present model.

Both the elastic and the damping terms in (5) are an indirect measure of EMGs in (6). At the final stage of muscle torque output, therefore, the graded torque development of a muscle torque must be considered. This process is modeled based on the fact that the contractile force curve due to the current stimulation is quite close to that of a critically damped second-order system

$$\ddot{\tilde{\tau}} + 2\psi^{-1}\dot{\tilde{\tau}} + \psi^{-2}\tilde{\tau} = \tau \qquad (7)$$

where $\tilde{\tau}$ represents instantaneous torque. ψ is a time-constant set to 15msec as suggested by Gribble et al. (1998) based on the empirically observed times from the onset of stimulus to maximum force in the human adductor pollicis muscle (Hainaut et al., 1981).

3.7. Limb Dynamics

The dynamics of the forearm is described by

$$\ddot{x} = I^{-1}\tilde{\tau} \tag{8}$$

where I is the sum of moment of inertia of the forearm and manipulandum, assumed as a rigid body hinged with the fixed center of rotation of the elbow joint. The I value in (8) varied among subjects (Table 1). The moment of inertia of the forearm was derived from the regression equations based on various length and circumference measurements of the segment, developed for cadaver populations (Hinricks, 1985). That of the manipulandum alone (aluminum plate: specific gravity 2.71 g, total weight 586.3 g, length 0.4 m) was estimated as 0.0313 kgm^2. Numerical integrations were performed on the left side to obtain current joint velocity ($\dot{x}$) and position (x).

4. Results

In each task for simulations, the variation of measured displacement curves for 15 trials were visually inspected to ascertain whether the corresponding average was appropriate to represent the 15 trials. For example, typical recordings for 15 displacement curves in the L movement with normal condition, load condition and relaxed condition are presented in Figs. 2A–C, respectively. In three conditions in Fig. 2, although some inter-trial variability can be seen in the individual curves, the characteristic features of movements are essentially preserved in the corresponding averaged data, shown in Fig. 3C(1), Figs. 7A and Fig. 8A, respectively.

4.1. Pulse Dependent Simulation

Figure 3 shows three sets of measured and simulated movements in the normal condition. Measured movements performed for different distances are simulated by varying the height (a) and width (t_2) of the V command, i.e., a/t_2 is 324/52, 377/97 and 516/100 for S, M and L movement, respectively. The model accounted for the following qualitative and quantitative features of measured kinematics. The movement of greater distance is associated with the increase of peak velocity achieved [panels (2)]. The faster movement provokes larger first overshoot in the displacement curves [pan-

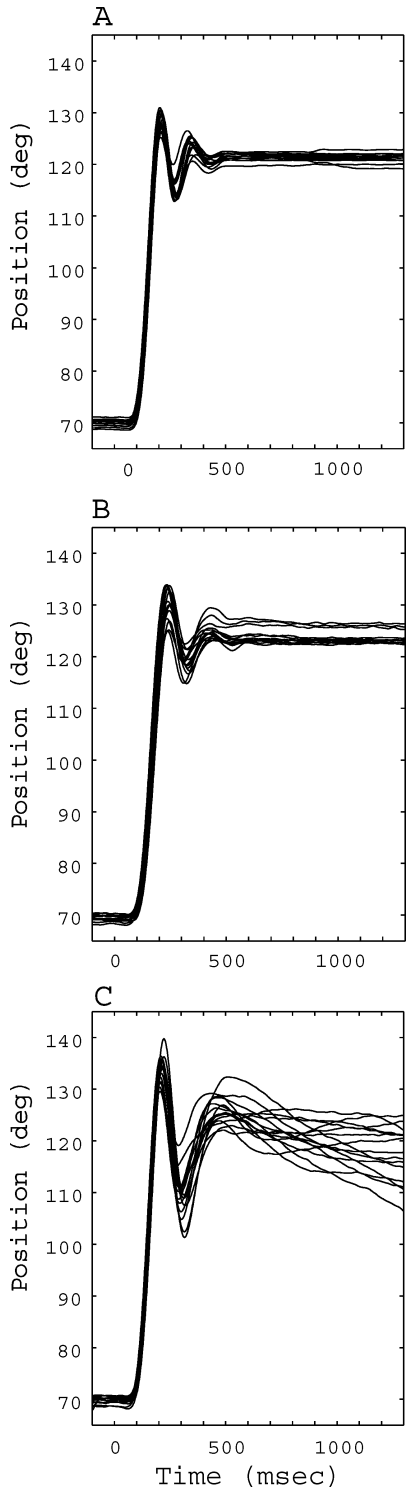

Figure 2. Joint displacement curves obtained for the large (50°) movement with three different task conditions (A: normal condition; B: load condition; C: relaxed condition). In all conditions, 15 trials performed by the same subject are superimposed.

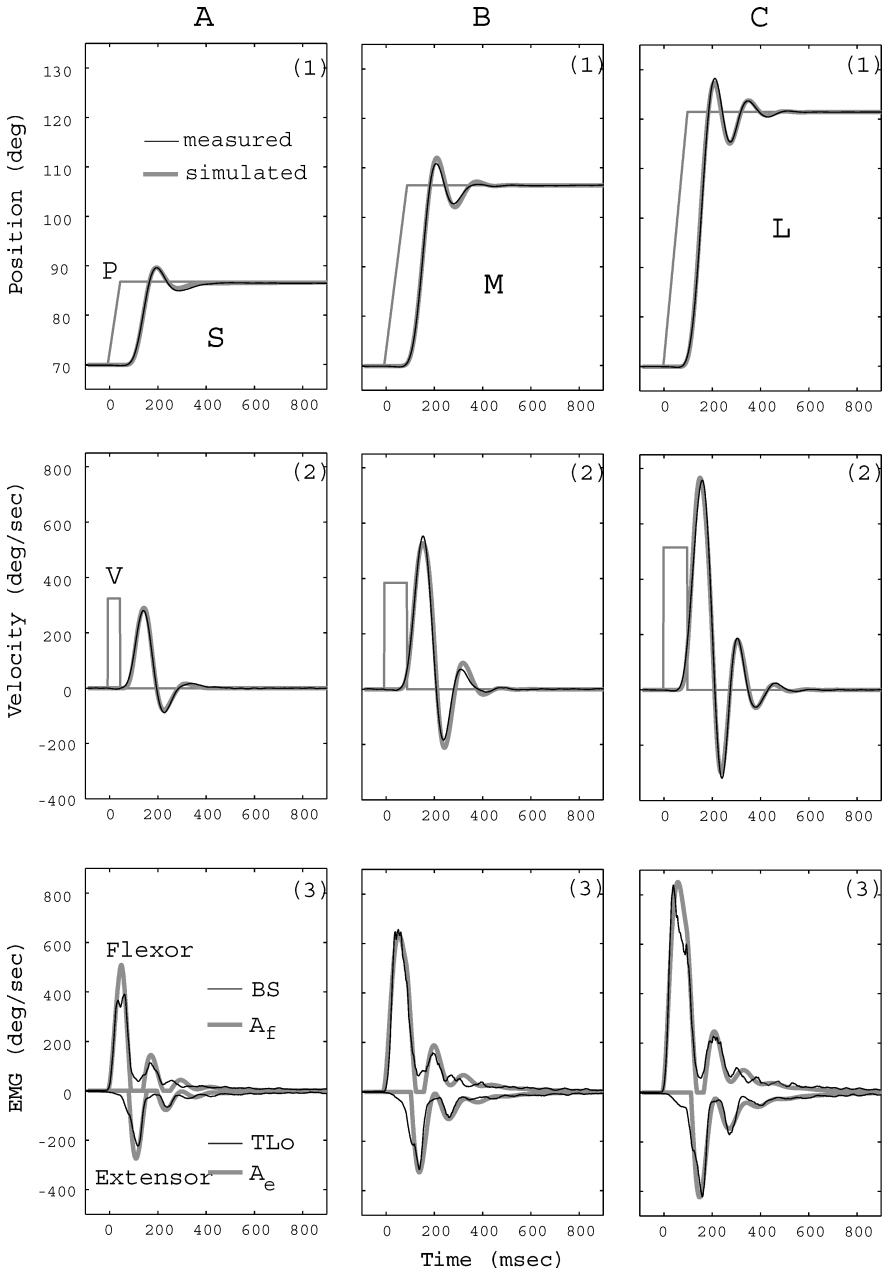

Figure 3. Measured and simulated movements in the normal condition with *S* (A, left column), *M* (B, middle column) and *L* movement (C, right column). First (1), second (2) and third row (3) represent the displacement curves, velocity curves and EMGs, respectively. Measured data in all panels are represented by the average of 15 trials. In each panel, a simulated curve (half-tone line) is superimposed on the corresponding measured curve (solid line). In each condition, *V* command and the corresponding *P* command with the best-fit parameters (i.e., $t_2$and a) are depicted by half-tone lines in panels (2) and (1), respectively.

els (1)]. The subsequent oscillations estimated from the first velocity zero-crossing are damped within 1 cycle in the *S* movement [A(2)] and 2 cycles in the *L* movement [C(2)]. The rates of these oscillations (estimated separately for each successive half-cycle) varied in the range of 5.5 to 7.8 Hz, and averaged 6.5 Hz across the three conditions. The number and the rate of terminal oscillation resembled those reported in a series of wrist joint studies by Milner and colleagues (Milner, 2002; Milner and Cloutier, 1998).

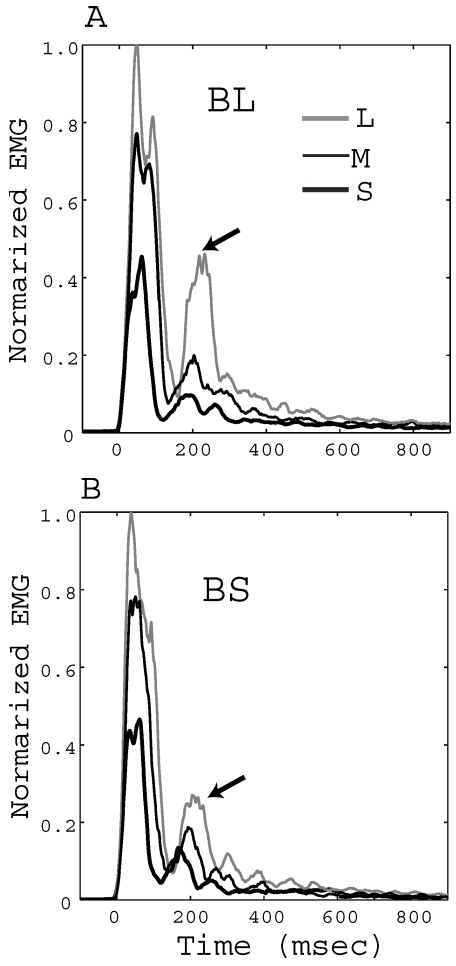

Figure 4. Comparison of the measured EMG profiles of synergist muscles. EMGs of BL and BS muscles in three movement distances (i.e.,*S*, *M* and *L*) are superimposed in A and B, respectively. EMGs are scaled with respect to the peak value of the large (50°) movement. Arrow in each panel indicates the second agonist burst.

Alternating activations of antagonistic muscles (BS and TLo) were well represented by the model (A_f and A_e, respectively) in terms of their rythmicity and gradual decay with time [panels (3)]. The agonist (flexor: BS) burst showed an initial high peak, followed by an intermittent depression and subsequent second much lower bursts. The amplitude and duration of the first agonist burst both increased with movement distance, implying that the magnitude of this burst is modulated burst-height and burst-width dependently (see also Fig. 4). Correspondingly, the amplitude and duration of the first agonist burst of the model varied in association with the changes of height (a) and width (t_2) of the V command, respectively [see rectangular pulses in panels (2)], as they lead to variations in amplitude and width of the initial half-cycle of the command x_r, respectively (Fig. 1A).

As can be seen in the temporal relationship between velocity curves [panels (2)] and alternating EMG bursts in the three movement conditions [panels (3)], the mechanical oscillations were accompanied by phase-locked alternating muscle activity superimposed on the underlying tonic muscle activation. The model accounted for this relationship in three conditions. In EMGs, a short-lasting oscillatory burst with a few cycles has often been recorded at the end of rapid elbow single-joint (Hore et al., 1991; Suzuki et al., 2001; Yamazaki et al., 1993) and wrist single-joint movements (e.g., Milner, 2002; Milner and Cloutier, 1998; Topka et al., 1999). After this, stable coactivation is manifested toward the complete relaxation of the limb (see also Gribble and Ostry, 1998; Milner, 2002; Milner and Cloutier, 1998; Suzuki et al., 2001; Yamazaki et al., 1994). The model predicts that in the corresponding phase there is no reciprocal facilitation or inhibition to the opposing muscles, both of which activities decay symmetrically.

Since the best-fit parameters (a and t_2) of the model were derived by reproducing measured displacement curves (see Methods), the model prediction of the measured data (i.e., mean of three distances of 4 subjects, $n = 12$) was degraded from displacement data ($r^2 = 0.991$), velocity data ($r^2 = 0.946$) to EMG data at most (A_f-BS, $r^2 = 0.741$; A_f-BL, $r^2 = 0.650$; A_e-TLo, $r^2 = 0.488$; A_e-TLa, $r^2 = 0.525$) (Table 1). Co-variation of correlation with movement distances was not found between the analyzed variables (displacement curves, $r^2 = 0.997, 0.990, 0.987$; velocity curves $r^2 = 0.971, 0.919, 0.946$; EMGs, A_f-BS, $r^2 = 0.719, 0.714, 0.790$; A_f-BL, $r^2 = 0.542, 0.637, 0.769$; A_e-TLo, $r^2 = 0.360, 0.436, 0.670$; A_e-TLa, $r^2 = 0.410, 0.410, 0.755$ for L, M and S conditions, respectively) (Table 1). Model predictions of extensor EMGs were degraded compared to the flexor EMGs (mean of 4 subjects × 2 muscles × 3 distances, $r^2 = 0.695$ for flexors; $r^2 = 0.507$ for extensors). A further difference in the model predictions can be seen in the EMGs of the synergists (mean of 4 subjects × 3 distances, $r^2 = 0.741$ for BS; $r^2 = 0.650$ for BL; $r^2 = 0.488$ for TLo; $r^2 = 0.525$ for TLa). The origin of this error can be found in the measured EMGs in Fig. 4, in which BL shows partial discrepancy to BS burst in the L movement, having a second BL burst greater than that of the BS burst (see arrows). Such differences in burst-height modulation among multiple

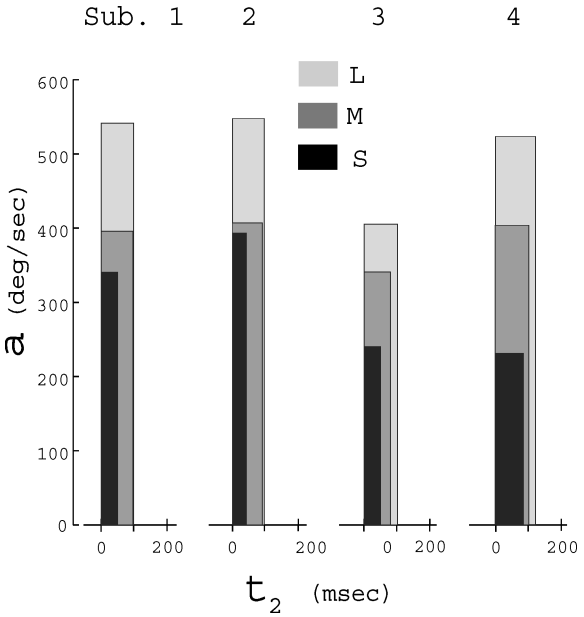

Figure 5. Comparisons of the V commands used for the simulations of four subjects. The height and width of a vertical column specify a and t_2 of the V command, respectively. Each set of three vertical columns presents the rectangular pulse of the V command used for the best-fit simulation of large (L), medium (M) and small (S) movements, performed by a single subject.

bursts were frequently seen in both of the flexor and extensor synergist muscles.

The model with an altered pulse-height/pulse-width paradigm in scaling the V command covers the subject-dependent variation of the measured kinematics and EMGs. Figure 5 represents the relationship between height (a) and width (t_2) of the V command used for the best-fit simulation in three conditions of all subjects (for displacement curves; $r > 0.99$, $p < 0.001$) (see Table 1). Obviously, trends in scaling magnitude of the V command with increase of movement distance differ among subjects. For example, the V command used for the simulation of subjects 1 and 2 shows pulse-width dependent modulation from S to M movement, but pulse-height dependence from M to L movement. In contrast, in subjects 3 and 4 the pulse-height and pulse-width co-vary with movement distances.

4.2. *Combined Effects with Pulse-Height and Pulse-Width Control*

In order to feature the effect of the pulse parameters of the V command on the scaling of kinematics and EMGs, two sets of simulations were conducted in Fig. 6A and 6B, in which either of pulse-height (a) or pulse-width (t_2) was changed while the other was fixed in three movement distances. The same model and same movement distances as those in Fig. 3 were used. In these simulations, the manner in which either of the height or width of the initial agonist burst are modulated to generate the class of scaled movements is consistent with the concept of two modes of control strategies (pulse-height and pulse-width control) as follows.

In Fig. 6A, t_2 is constant at 100 msec for all tasks, such that pulse-height a increases in proportion to the movement distance ('pulse-height control'), i.e., a is 169, 366 and 516 deg/sec in S, M and L movements, respectively. The magnitude of the EMG bursts of antagonistic muscles [A(2)] increases in association with the pulse-height a[A(1)]. Qualitative features of EMGs are not altered by the pulse-height, such that a greater pulse-height elicits quicker and greater bursts in both A_f and A_e bursts while keeping their peak timings and durations nearly constant. This burst-height dependent modulation of EMGs is accompanied by the increase of peak velocity, implying that the pulse-height control is linked to the speed control of the system. The characteristic modulations of EMGs and kinematics well accounted for the behavioral data from elbow (Corcos et al., 1989; Hallet and Marsden, 1979; Yamazaki et al., 1993) or wrist single-joint movements (Hoffman and Strick, 1990; Freund and Büdingen, 1978).

A second set of simulations (Fig. 6B) was conducted to produce scaled movements of different distances by keeping a constant at 516 deg/sec while altering the t_2 value to 33, 71 or 100 msec in S, M and L conditions, respectively ('pulse-width control'). As the t_2 value increases, the first A_f burst is elongated to have a greater area with movement distance, whereas the initial part of the first A_f bursts shows the same activation curve in three conditions [B(2)]. Similarly, velocity curves are not changed early in the trajectory, taking the same curve initially and deviating from it as they are elongated with t_2 value [B(1)]. Interestingly, the peak of the first A_f burst from M to L movement is not affected by t_2 [B(2)]. The same is true for the peaks in the corresponding velocity curves [B(1)]. As t_2 increases, the first A_e burst is delayed with the end of the first A_f burst [B(2)] and its peak is slightly reduced from M to L movement condition (upward arrow). The same is true for the second A_f burst (downward arrow). These non-monotonic modulations of EMG and

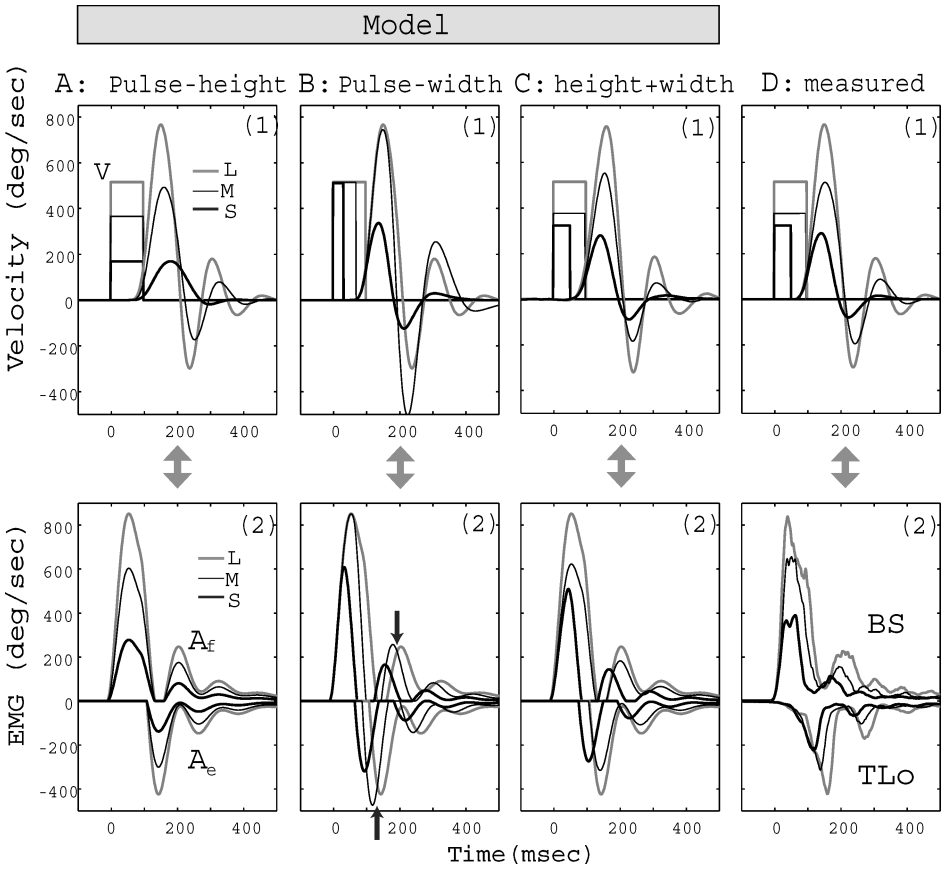

Figure 6. The pulse-height and pulse-width control, and their relative contributions to the simulation of the experimental data in Fig. 3. First row (1)s are V commands and resulting velocity curves, and second row (2)s are EMGs of the antagonistic muscles. In each panel, variables for the large (L), medium (M) and small (S) movement are depicted by half-tone line, thin-line and thick-line, respectively. A: pulse-width is fixed while pulse-height is varied alone, and vice versa in B. C: combined effects of pulse parameters on the simulation of the measured data in D. Note that the movement distances used in all of the simulation data (A, B and C) are equal to those of the measured data in D. For explanation of arrows and symbols, see the text.

velocity curves with movement distance can be seen in behavioral data, of which the speed was not explicitly controlled to move a greater distance (Berardelli et al., 1984; Cheron and Godaux, 1986; Hoffman and Strick, 1990; Gottlieb et al., 1996; Pfann et al., 1998; Suzuki et al., 1994).

The control scheme behind the measured data in Fig. 3 shares both the features in the pulse-height (Fig. 6A) and pulse-width control (Fig. 6B). Figure 6D1 and 6D2 show the sets of measured velocity curves and EMGs, respectively. Corresponding simulations are shown in C(1) and C(2), respectively. In Fig. 6C, since pulse-width (t_2) is elongated from S to M movements with minor changes of pulse-height (a), the scaled movement distance is mainly associated with the increase in pulse-width (t_2). From M to L movement, in contrast, the scaled movement distance is dependent on the pulse-height (a). The combined effect of pulse-width and pulse-height control in C(2) reflects the same scaling of the movements shown in A(2) and B(2), respectively. From S to M movement, for example, a greater first A_f burst is achieved by elongating the duration and simultaneously delaying the onset of the first A_e burst. This mirrors the case when pulse-width is varied alone in B(2). Associated with this is a common initial slope of velocity curve in B(1). From M to L movement, the first A_f burst diverges from the earliest moment of the movement, while keeping the duration nearly constant. This mirrors the case when pulse-height was varied alone in A(2).

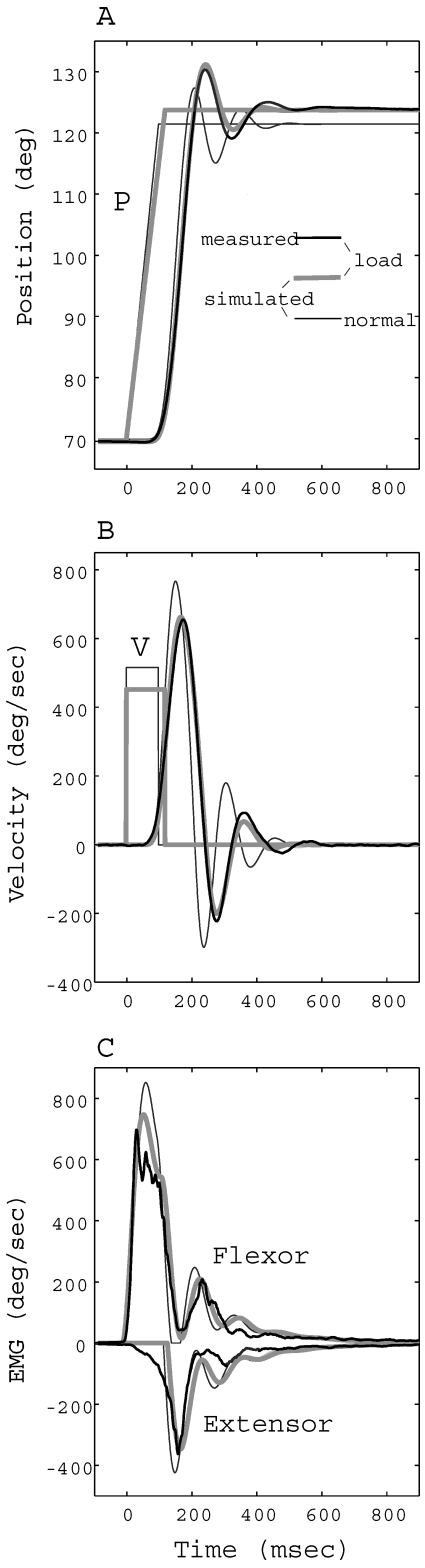

Figure 7.

4.3. *Effects of Inertial Load*

The model prediction for L movement in the load condition is illustrated in Fig. 7, where the same subject and model as in Fig. 3 are used in the simulation. In each panel, simulated curves for the load condition are superimposed on the measured data, together with simulation curves obtained in the normal condition in Fig. 3. In the load condition, the simulated movement accounts for the measured displacement (A) and velocity curves (B) quite well. The simulated EMGs provide good agreement with the first agonist and first antagonist burst (C), while after these the discrepancy between the measured and simulated EMGs become manifest.

The best-fit model parameters of the V command in the load condition were 459 deg/sec and 118 msec for a and t_2, respectively. Thus the height (a) and width (t_2) of the V command in the simulation of load condition are reduced and increased, respectively, with respect to those used in the simulation of normal condition (compare the pulse shapes in the two conditions in B). By this effect, the initial agonist EMG burst in the load condition is prolonged slightly, and the subsequent alternating bursts lag behind that of the normal condition (C). Also, the inertial load effect slowing the movement is apparent in the simulation of load condition, that is, the rate of rise of displacement curve (A) and peak velocity time in the load condition (B) are lower and later, respectively, than those of the simulated curves in the normal condition. Also evident from the simulated velocity curves (B) is that the rate and amplitude of terminal oscillation in the loaded condition are slower and lower, respectively, than those of the normal condition.

4.4. *Effects of Reduced Coactivation*

The model predictions for L movement in the relaxed condition are represented in Fig. 8, together with simulation curves in the normal condition in Fig. 3. In the relaxed condition, the level of coactivation command was simply reduced to a half (i.e., $0.5a$) of that used in the simulation of the normal condition. In the

Figure 7. Model prediction for the effects of inertial load on the kinematics and EMGs. Panels A, B and C are for the displacement curves, velocity curves and EMGs, respectively. In the three panels, thick line and half-tone lines represent the measured and simulated curves in the load condition, respectively, and thin lines are for the simulated curve in the normal condition in Fig. 3.

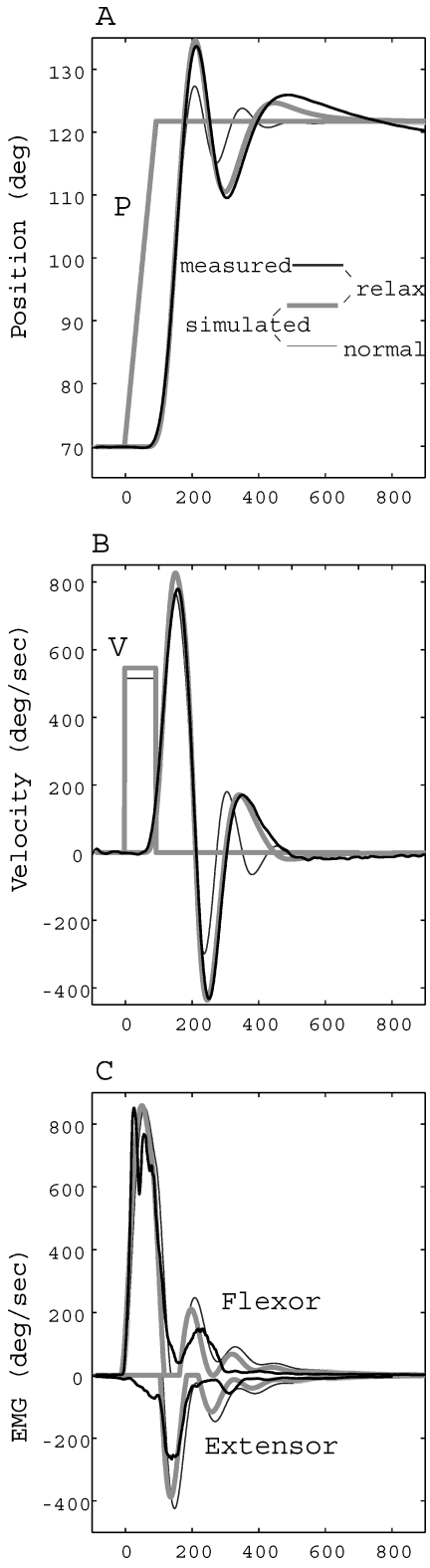

Figure 8.

relaxed condition, the simulated movement accounts for the measured displacement (A) and velocity curves (B) quite well. As for EMGs, the simulated EMGs provided good agreement with the first agonist and first antagonist burst (C), while after these the rate of oscillation of the simulated EMGs was higher than that of the measured EMGs.

The best-fit V parameters a and t_2 of the model for the relaxed condition were 546 deg/sec and 95 msec, respectively, both of which are nearly consistent with those of the normal condition (compare the pulse shapes in the two conditions in B). By this effect, the simulated EMG for the first agonist burst in the relaxed condition takes a shape almost comparable to that of the simulated one in the normal condition (C). Correspondingly, both the initial slope of the simulated displacement curve (A) and the initial half-cycle of the simulated velocity curve (B) are almost equivalent in two conditions. After the initial agonist burst, however, the difference of the two conditions becomes manifest in the reduction and phase lead of alternative burst of EMGs in the relaxed condition, with respect to the normal condition (C). In the simulated displacement curve, the weak coactivation in the relaxed condition causes a larger overshoot, and slow but large drawback at the final position, followed by slow curve (A) (see also Fig. 2C). Correspondingly, the velocity curve in the relaxed condition exhibits slower and larger negative and positive overshoots about the zero-velocity than those of the normal condition (B). Thus the rate of oscillation in the relaxed condition is apparently lower than that of the normal condition (compare the timings of multiple peaks in velocity curves during terminal oscillation in B).

5. Discussion

5.1. Comparisons to Oculomotor Control

Our subjects showed a combined feature of pulse-height and pulse-width control to move with a greater

Figure 8. Model prediction for the effects of the reduced coactivation command on the kinematics and EMGs. Panels A, B and C are for the displacement curve, velocity curve and EMGs, respectively. In the three panels, thick line and half-tone lines represent the measured and simulated curves in the relaxed condition, respectively, and thin lines are for the simulated curve in the normal condition in Fig. 3. In A, note that the P curve used for the simulation in the normal condition is behind that in the relaxed condition and thus invisible.

distance (e.g., Fig. 6D). The corresponding simulations revealed that the pulse-height and pulse-width control of the initial agonist EMG were attributable to the V command parameters, which were weighted for either height (a) or width (t_2) under different distance conditions, respectively (Fig. 6C). Although these two modes of control strategies in the model were developed based on the saccade in the oculomotor system, the differences of pulse-dependent control in the two systems might be noted as follows.

First, in the skeletomotor system the duration of the first agonist burst can be lengthened whenever there is a need to extend the time course of the initial propulsive force (Gottlieb, 1996; Gottlieb et al., 1989; Hoffman and Strick, 1990, 1993). By contrast, modification of the pulse-width of oculo-MN discharge is limited to the case where the angular distance to move exceeds a certain limit (Evinger and Fuchs, 1978; Fuchs and Luschei, 1970). This means that the origin of the difference between the control of two systems is that the subjects are able to control volitionally the velocity of the limb, but lack volitional control over the velocity of a saccade.[3] According to the series of wrist movement studies performed by Hoffman and Strick (1990, 1993), two control strategies (pulse-height and pulse-width) are combined into a set of control patterns depending on the various task requirements, such as speeds, distances or loads. Clearly, our experimental results and their simulation model are along this line, that is, the height and width of the pulse command can be controlled (or adjusted) independently over the entire workspace and time, and these effects reflect the concomitant pattern of modulation of the first agonist burst and velocity (Fig. 6). Furthermore, an accuracy constraint or additional loading for the limb segment provokes a long-duration agonist burst even for movements where the amplitude of the movement is kept constant (Gottlieb, 1996; Hoffman and Strick, 1990, 1993; Pfann et al., 1998) (for our result, see Fig. 7). The same adaptive flexibility in the adjustments of agonist MNs discharges cannot be expected in the saccadic movements of the oculomotor system.

Second, in the oculomotor system the pulse command reflects the pattern of agonist oculo-MN discharge only. On the other hand, limb movements are associated with alternating bursts and subsequent coactivation of antagonist muscles. This might be considered as evidence that control of the skeletomotor system is different from the oculomotor system. However, since the inertia of the eye is negligible and thus the generation of braking and/or damping force for eye movements depends largely on the inherent viscoelastic resistance of the plant, the antagonist eye muscles are weakly active or silent during the course of movement (Robinson, 1970). In contrast, a limb involves more inertia than an eye, so as the speed of movement is increased a braking force in the antagonist muscle and an effective damping or cramping force due to coactivation may both be specifically needed in order to realize accurate positioning of the limb at the end point (e.g., Ghez and Martin, 1982; Gottlieb, 1996; Hoffman and Strick, 1993). In agreement with previous reports (Freund and Büdingen, 1978; Ghez and Martin, 1982; Robinson, 1986; Hoffman and Strick, 1993), therefore, it appears that there is no difference in terms of the basic ways in which control signals acts to produce limb and eye movements. Rather it is likely that control of the two systems may be largely affected and specialized by the plant mechanics peripheral to the control system.

5.2. *Pulse-Based Expansion of the Equilibrium Point Hypothesis*

The significance of the alternating activation and coactivation of the antagonistic muscles for the control of single-joint movements may be considered within the framework of the present model, as follows.

The equilibrium point shift x_p is represented by the time integral of the reciprocal command x_r. This implies a 90° phase lead of x_r with respect to the x_p curve, implying that flexor and extensor stiffness are elevated significantly during the flexion and extension phases of the equilibrium point shift, respectively. Thus the velocity-dependent organization of reciprocal activation would lead to the phase-locked elevation of muscle stiffness with equilibrium point shift. The alternating muscle bursts in the model are also considered while taking into account the state-dependency of damping force of the active muscle. When the equilibrium point is moved ahead in a single stroke of elbow flexion, flexor stiffness transforms a displacement from the equilibrium point into an elastic restoring force. However, the damping related to the increase of the shortening velocity of this muscle would reduce the elastic torque elevated initially (negative effect). Therefore, an initial strong pulse-like EMG burst of the agonist muscles (flexor) would be needed to compensate for this reduction (see Gottlieb, 1996). On the other hand, in the same phase while the elbow is still being

flexed, the dynamic situation of the opposing (extensor) muscles would be reversed. The extensor EMG would lead to the effective damping of this lengthened muscle without apparent elevation of excitation (positive effect). These opposite damping effects in a single stroke of movement would lead to the programming of asymmetric activation signals during movement, i.e., large first agonist burst and small first antagonist burst. Thus asymmetry between the agonist and antagonist activity in the measured data, which was predicted in the simulation data, might be a natural consequence of different situations of these muscles for damping (Gottlieb, 1996).

The coactivation command in the model would modify the damping scheme above in a more efficient way. The command x_c elevates the initial agonist burst more than that produced by the initial half-cycle of the command x_r alone (Fig. 1A and C). By this effect, the output force of the agonist (flexor) muscles would be elevated to compensate for the reduction of force arising due to the muscle shortening. After the peak of an initial half-cycle of x_r, the command x_c leads to the earlier onset of the opposing muscles' excitation to overlap with the end of the agonist burst (Fig. 1A and C). By this effect, the braking force of the antagonist (extensors) muscles may increase earlier than in the case without coactivation, leading to the effective damping (or braking) of the movement. As for the latter mechanism, the overlap of the antagonistic muscles' excitation become manifest toward the movement end, followed by coactivation after the movement end (Fig. 3). This means that successive braking actions of opposing muscles would be blended and then dominated by the cocontraction of these muscles. This would lead to stabilization of the limb by clamping it at the final equilibrium position (Lacquaniti and Maioli, 1989; Milner, 2002). Supporting evidence can be seen in the comparison of the movements with normal and relaxed conditions in Fig. 8, which implies that the coactivation command would be needed to limit an overshoot and then stabilize the limb at the final equilibrium position.

Based on the previous empirical observations (Milner and Cloutier, 1993; Bennet, 1993; Suzuki et al., 2001), our model assumed a speed-related linkage of reciprocal command and coactivation command. In our experiment, however, measured movement in the relaxed condition yielded selective depression of coactivation, and the model with a low gain coactivation command replicated this movement under the corresponding instruction (Fig. 8). Using the same instructions to subjects, Yamazaki et al. (1994) have shown that coactivation almost disappeared, while the essential features of reciprocal activation were preserved with very short overlap of activation of the antagonistic muscles. These results suggest that the coactivation command is not tightly linked to the reciprocal command, but rather coactivation is separately modifiable depending on the task requirements. As a related matter, previous works have shown that subjects tend to reduce the level of coactivation as they learn to move with a novel task (Burdet et al., 2001; Milner, 2002; Milner and Cloutier, 1998). This is regarded as the key element of motor learning (Osu et al., 2001; Thoroughman and Shadmehr, 1999).

5.3. Limitations of Reflex-Dependent Modulation

Our model is based on the assumption that the descending commands (V) contribute to muscle activation (x_r, x_c) at all times from the beginning to the end of terminal oscillation, whereby reflex-dependent generation (or modification) of the EMGs, elastic and damping torque are not assumed at all. In Fig. 6, supporting evidence for this assumption may be found in the temporal relationship between EMGs [D(2)] and kinematics [D(1)] in the measured data, in which both of the first antagonist burst and the second agonist burst occur before (or at least at the same time as) the positive and negative phase of the velocity curves, respectively. Taking into account the fixed reflex delays of 20–30 msec in the upper arm muscles (Lacquaniti and Maioli, 1989; Wolf and Segal, 1996), these successive reciprocal bursts of the antagonist muscles may not be initiated by the stretch reflex, but rather reflect pre-programmed activity that is sent out by the higher control center (Berardelli et al., 1996).

The effectiveness of the reflex contribution to the control of fast limb movements is still questionable in both of the behavioral (Milner and Cloutier, 1993) and theoretical terms (Hogan et al., 1987; Mussa-Ivaldi and Bizzi, 2000). The common explanation for this is that reflexively elicited muscle activation and forces would be late following the intrinsic muscle mechanical response, causing system instability. Milner and Cloutier (1993) have demonstrated this in the wrist joint, and suggested that 6–7.5 Hz could be the critical frequency range of motion provoking reflex instability (see also Milner and Cloutier, 1998). However, even though terminal oscillation in rapid, well-practiced voluntary movements could be performed in these critical frequency ranges, reflex instability (or oscillation) never

happened, as also confirmed in this study (Fig. 3). The main reason for this may be that the torque contributed by the predictive control of active muscles completely dominates any torque due to stretch reflex (Milner and Cloutier, 1993), and/or that the reflex itself is centrally suppressed during limb movements (Gottlieb and Agarwal, 1980; Hallet et al., 1975; Soeching et al., 1981). As for the latter mechanism, Seki et al. (2003) found that descending motor commands inhibit the sensory input to the spinal cord presynaptically before and during the arm movement.

Since terminal oscillation manifests as the speed of movement increases (e.g., see Fig. 3), a speed-related increase of post-movement coactivation will be needed (Milner, 2002; Suzuki et al., 2001). This would increase the joint stiffness and thereby limit oscillation of the limb within a small amplitude range (Milner, 2002). However, an increase of the joint stiffness is accompanied by an increase in the natural frequency of elastic oscillation of the limb (Milner and Cloutier, 1993). This can be seen in the comparison of the rate of terminal oscillation between normal and relaxed conditions in Fig. 8. The terminal oscillations in the normal condition were in the range of 5.5 to 7.8 Hz, and averaged 6.5 Hz in three conditions. Within this frequency range, the additional participation of the reflex damping might be problematic, because, as described above, the stretch reflex has a limited capacity for braking and damping of high frequency movements (Milner and Cloutier, 1993; Rack, 1981). Instead, therefore, damping of the terminal oscillation might be achieved by the underlying coactivation without apparent participation of the stretch reflex (Rack, 1981).

5.4. Concluding Remarks

The center of the present model is a single rectangular velocity (pulse) command. The derivations of equilibrium point shift, muscle control inputs, elastic and damping torque, are straightforward as they are scaled by the height and width of the velocity command alone. The system dynamics depends on the parametric specifications of the velocity command alone, without the need for explicit computations of muscle control actions, such that the restoring forces are realized as an implicit interaction among the moving equilibrium point, mechanical properties of active muscles and kinematics. This means that the model is still kinematics-dependent, and is independent from the problems of state-dependency of muscle force generation, which must be taken into account in the programming of control actions when using inverse dynamics approaches. The argument for simplicity of control does hold in the situation in which the control system would need simplicity the most.

Acknowledgments

The authors thank Dr. D. J. Ostry, Dept. of Psychology, McGill University, for his critical comments on an earlier version of this manuscript, based on his profound insight about the equilibrium point hypothesis. This study was supported by Kinjo Gakuin University-Parent Teacher Association Special Research Subsidy.

Notes

1. According to Brooks and Thach (1981), the precentral cell assembly could compose the initial pulse according to the motor plan. During and at the end of the movement, appropriate combinations of neurons could also assist in adjusting bursts for the agonist and antagonist muscles. Such timing of alternative activation of the antagonist muscles is thought to depend on the ability of the cerebellum to trigger the motor cortex at the appropriate times, with minor contribution of stretch reflex (see also review of Berardelli et al., 1996).
2. In Cannon and Zahalak (1982), the elbow joint stiffness during sinusoidal perturbation increases linearly and approaches 250 Nm/rad with background torque from rest to maximal voluntary contraction. The SPUT value is 4–7 Nm/rad, comparable to 6 ± 1.1 Nm/rad reported by Bennet (1993) using a step perturbation at the instant of elbow single-joint movement, and 6.27 Nm/rad by Osu et al. (2001) used in the present model.
3. According to Evinger and Fuchs (1978), eye movements of cats to a visual target are characterized by a sharply accelerating initial segment of roughly constant duration. The durations of both oculo-MN discharge and the resulting eye movement are constant for saccades below about 10 degrees. The frequency of oculo-MN discharge and speed of movement are modulated to vary the amplitude of small saccades in which, the larger the angular distance moved, the higher the maximum velocity achieved. In contrast, eye movements of greater than about 10 degrees are generated by nearly maximal, high frequency bursts of activity in the agonist oculo-MNs, hence larger amplitude saccadic eye movements have a significantly longer duration than smaller amplitude saccades, and the peak velocity of larger saccades increases only slightly over that of small movements (see also Fuchs and Luschei, 1970).

References

Barto AG, Fagg AH, Stikoff N, Houk JC (1999) A cerebellar model of timing and prediction in the control of reaching. Neural. Comp. 11: 565–594.

Bennet DJ (1993) Torques generated at the human elbow joint in response to constant position errors imposed during voluntary movements. Exp. Brain Res. 95: 488–498.

Berardelli A, Hallet M, Rothwell JC, Agostino R, Manfredi M, Thompson PD, Marsden CD (1996) Single-joint rapid arm movements in normal subjects and in patients with motor disorder. Brain 119(2): 661–674.

Berardelli A, Rothwell JC, Day BL, Kachi T, Marsden CD (1984) Duration of the first agonist EMG burst in ballistic arm movements. Brain Res. 304: 183–187.

Bizzi E, Accornero N, Chapple W, Hogan N (1984) Posture control and trajectory formation during arm movement. J. Neurosci. 4(11): 2738–2744.

Bizzi E, Hogan N, Mussa-Ivaldi FA, Giszter S (1992) Does the nervous system use equilibrium-point control to guide single- and multiple joint movements? Behav. Brain Sci. 15: 603–613.

Braitenberg V, Heck D, Sultan F (1997) The detection and generation of sequences as a key to cerebellar function: Experiments and theory. Behav. Brain Sci. 20(2): 229–277.

Brooks VB, Thach WT (1981) Cerebellar control of posture and movement. In: Brooks VB, ed. Handbook of Physiology. The Nervous System. Motor Control. Am. Physiol. Soc., Bethesda, MD, Sect. 1, Vol II, pp. 877–946.

Burdet E, Osu R, Franklin DW, Milner TE, Kawato M (2001) The central nervous system stabilizes unstable dynamics by learning optimal impedance. Nature 414: 446–449.

Cannon SC, Zahalak GI (1982) The mechanical behavior of active human skeletal muscle in small oscillation. J. Biomech. 15: 111–121.

Cheron C, Godaux E (1986) Self-terminated fast movement of the forearm in man: Amplitude dependence of the triple burst pattern. J. Biophys. Biomech. 10: 109–117.

Corcos DM, Gottlieb GL, Agarwal GC (1989) Organizing principle for single-joint movements. II. A speed-sensitive strategy. J. Neurophysiol. 62: 358–368.

DeLuca CJ, Mambrito B (1987) Voluntary control of motor units in human antagonist muscles: Coactivation and reciprocal activation. J. Neurophysiol. 58: 525–542.

Evinger C, Fuchs AF (1978) Saccadic, smooth pursuit and optokinetic eye movements of the trained cat. J. Physiol. (Lond.) 285: 209–229.

Feldman AG, Adamovich SV, Ostry DJ, Flanagan JR (1990) The origin of electromyogram- Explanation based on the equilibrium point hypothesis. In: JM Winter, SL-Y Woo, eds. Multiple Muscle Systems: Biomechanics and Movement Organization. Springer-Verlag, New York, pp. 195–213.

Flash T (1987) The control of hand equilibrium trajectories in multi-joint arm movements. Biol. Cybern. 57: 257–274.

Freund H-J, Büdingen HJ (1978) The relationships between speed and amplitude of fast voluntary contraction of human arm muscle. Exp. Brain Res. 31: 1–12.

Frysinger RC, Bourbonnais D, Kalaska JJ, Smith AM (1984) Cerebeller cortical activity during antagonist cocontraction and reciprocal inhibition of fore-arm muscles. J. Neurophysiol. 51: 32–49.

Fuchs AF, Luschei ES (1970) Firing patterns of abducens neurons of alert monkeys in relationship to horizontal eye movement. J. Neurophysiol. 33: 382–392.

Ghez C (1979) Contributions of central programs to rapid limb movement in the cat. In: H Asanuma, VJ Wilson, eds. Integration in the nervous system. Igaku-Shoin, Tokyo, pp. 305–320.

Ghez C, Martin JH (1982) The control of rapid limb movement in the cat. III. Agonist-antagonist coupling. Exp. Brain Res. 45: 115–125.

Gielen CCAM, Houk JC (1984) Nonliner viscosity of human wrist. J. Neurophysiol. 52: 553–569.

Gomi H, Kawato M (1997) Equilibrium-point control hypothesis examined by measured arm stiffness during multijoint movement. Science 272: 117–120.

Gottlieb GL (1996) On the voluntary movement of compliant (inertial-visco-elastic) loads by percellated control mechanics. J. Neurophysiol. 76: 3207–3229.

Gottlieb GL, Agarwal GC (1980) Response to sudden torques about ankle in man. III. Suppression of stretch evoked responses during phasic contraction. J. Neurophysiol. 44: 233–246.

Gottlieb GL, Chen C-H, Corcos DM (1996) Nonlinear control of movement distance at the human elbow. Exp. Brain Res. 112: 289–297.

Gottlieb GL, Corcos DM, Agarwal GC (1989) Organizing principle for single-joint movements. I. A speed-insensitive strategy. J. Neurophysiol. 62: 342–357.

Gribble PL, Ostry DJ (1998) Independent coactivation of shoulder and elbow muscles. Exp. Brain Res. 123: 355–360.

Gribble PL, Ostry DJ, Sanguineti V, Laboissière R (1998) Are complex control signals required for human arm movement. J. Neurophysiol. 79: 1409–1424.

Grillner S (1981) Control of locomotion in bipeds, tetrapods, and fish. In: VB Brooks, ed. Handbook of Physiology. The Nervous System. Motor Control. Am. Physiol. Soc., Bethesda, MD, Sect. 1, Vol II, pp. 1171–1236.

Hainaut K, Duchateau J, Desmedt J (1981) Differential effects on slow and fast motor units of different programs of brief daily muscle training in man. In: Desmedt ed. Progress in Clinical Neurophysiology. Motor unit Types, Recruitment and Plasticity in Health and Disease, Karger, Basel, Vol 9, pp. 241–249.

Hallet M, Marsden CD (1979) Ballistic flexion movements of the human thumb. J. Physiol. (Lond) 294: 33–50.

Hallet M, Shahani BT, Young RR (1975) EMG analysis of stereotyped voluntary movements in man. J. Neurol. Neurosurg. Psychiatry 38: 1154–1162.

Hinricks RN (1985) Regression equations to predict segmental moments of inertia from anthropometric measurements: An extension of the data of Chandler et al. (1975). J. Biomech. 23: 949–951.

Hoffman DS, Strick PL (1990) Step-tracking movements of the wrist in humans. II. EMG analysis. J. Neurosci. 10: 142–152.

Hoffman DS, Strick PL (1993) Step-tracking movements of the wrist in humans. III. Influence of changes in load on patterns of muscle activity. J. Neurosci. 13: 5212–5227.

Hogan N (1985) The mechanics of multi-joint posture and movement control. Biol. Cybern. 52: 315–332.

Hogan N, Bizzi E, Mussa-Ivaldi FA, Flash T (1987) Controlling multijoint motor behaviors. Exer. Sport Sci. Rev. 15: 153–190.

Hore J, Wild B, Diener H-C (1991) Cerebellar Dysmetria at the elbow, wrist and fingers. J. Neurophysiol. 65: 563–546.

Humphrey DR, Reed DJ (1981) Separate cortical systems for control of joint movement and joint stiffness: reciprocal activation and coactivation of antagonist muscles. In: JE Desmedt ed. Advances in Neurology. Motor Control Mechanisms in Health and Disease. Raven, New York, Vol 39, pp. 347–372.

Jankowska E, Padel Y, Tanaka R (1976) Disynaptic inhibition of spinal motoneurons from the motor cortex in the monkey. J. Physiol. (Lond) 258: 467–487.

Kearnery RE, Hunter IW (1990) System identification of human joint dynamics. CRC Crit. Rev. Biomed. Eng. 18: 55–87.

Lacquaniti F, Moioli C (1989) The role of preparation in tuning anticipatory and reflex responses during catching. J. Neurosci. 9: 134–148.

Lan N, Crago PE (1994) Optimal control of antagonist muscle stiffness during voluntary movements. Biol. Cybern. 71: 123–135.

Latash ML, Gottlieb GL (1991) Reconstruction of elbow joint compliant characteristics during fast and slow voluntary movements. Neuroscience 43: 697–712.

Latash ML, Goodman SR (1994) An equilibrium-point model of electromyographic patterns during single-joint movements based on experimentally reconstructed control signals. J. Electromyog. Kinesiol. 4: 230–241.

Milner TE (2002) Adaptation to destabilizing dynamics by means of muscle cocontraction. Exp. Brain Res. 143: 406–416.

Milner TE, Cloutier C (1993) Compensation for mechanically unstable loading in voluntary wrist movement. Exp. Brain Res. 94: 522–532.

Milner TE, Cloutier C (1998) Damping of the wrist joint during voluntary movement. Exp. Brain Res. 122: 309–317.

Mussa-Ivaldi, Bizzi E (2000) Motor learning through the combination of primitives. Phil. Trans R. Soc. Lond. 355: 1755–1769.

Osu R, Franklin DW, Kato H, Gomi H, Domen K, Yoshioka T, Kawato M (2001) Short- and long-term changes in joint co-contraction associated with motor learning as revealed from surface EMG. J. Neurophysiol. 88: 991–1004.

Osu R, Gomi H (1999) Multi-joint muscle regulation mechanism examined by measured human-arm stiffness and EMG signals. J. Neurophysiol. 81: 1458–1468.

Pfann KD, Hoffman DS, Gottlieb GL, Strick PL, Corcos DM (1998) Common principles underlying the control of rapid single degree-of-freedom movements at different joints. Exp. Brain Res. 118: 35–51.

Rack PMH (1981) Limitations of somatosensory feedback in control of posture and movement. In: VB Brooks, ed. Handbook of Physiology. The Nervous System. Motor Control. Am. Physiol. Soc., Bethesda, MD, Sect. 1, Vol. II, pp. 229–256.

Rack PMH, Westbury DR (1969) The effects of length and stimulus rate on tension in the isometric cat soleus muscle. J. Physiol. (Lond.) 204: 443–460.

Robinson DA (1970) Oculomotor unit behavior in the monkey. J Neurophysiol 33: 393–404.

Robinson DA (1986) Is the oculomotor system a cartoon of motor control. Progress in Brain Res. 64: 411–417.

Robinson DA (1989) Integration with neurons. Annu. Rev. Neurosci. 13: 33–45.

Rothwell JC, Day BL Berardelli A, Marsden CD (1984) Effects of motor cortex stimulation on spinal interneurons in man. Exp. Brain Res. 54: 382–384.

Seki K, Perlmutter SI, Fetz EE (2003) Sensory input to primate spinal cord is presynaptically inhibited during voluntary movement. Nature Neurosci. 6: 1309–1016.

Soechting JF, Dufrensne JR, Lacquaniti F (1981) Time-varying properties of myotatic responses in man during some simple motor tasks. J. Neurophysiol. 46: 1226–1243.

Suzuki M, Shiller DM, Gribble PL, Ostry DJ (2001) Relationship between cocontraction, movement kinematics and phasic muscle activity in single-joint arm movement. Exp. Brain Res. 140: 171–181.

Suzuki M, Yamazaki Y, Matsunami K (1994) Relationship between force and electromyographic activity during rapid isometric contraction in power grip. Electroencephalog. clinical Neurophysiol. 93: 218–224.

Thoroughman KA, Shadmehr R (1999) Electromyographic correlates of learning model of reaching movements. J. Neurosci. 19(9): 8573–8588.

Topka H, Mescheriakov S, Boose A, Kuntz R, Hertrich I, Seydel L Dichgans J, Rothwell J (1999) A cerebellar-like terminal and postural tremor induced in normal man by transcranial magnetic stimulation. Brain 122: 1551–1562.

Wadman WJ, Denier van der Gon JJ, Geuze RH, Mol CR (1979) Control of fast goal-directed arm movements. J. Hum. Mov. Stud. 5: 3–17.

Wolf SL, Segal RL (1996) Reducing human biceps brachii spinal stretch reflex magnitude. J. Neurophysiol. 75: 1637–1646.

Wu CH, Houk JC, Young KY, Miller LE (1990) Nonlinear damping of limb motion. In: JM Winter, SL-Y Woo, eds. Multiple Muscle Systems. Biomechanics and Movement Organization. Springer-Verlag, New York, pp. 214–235.

Yamazaki Y, Ohkuwa T, Itoh H, Suzuki M (1994) Reciprocal activation and coactivation in antagonistic muscles during rapid goal-directed movements. Brain Res. Bull. 34: 587–593.

Yamazaki Y, Suzuki M, Mano T (1993) Control of rapid elbow extension movement. Brain Res. Bull. 30: 11–19.